XI International Conference on Computational Plasticity. Fundamentals and Applications
COMPLAS XI
E. Oñate, D.R.J. Owen, D. Peric and B. Suárez (Eds)

SIMPLIFIED MULTISCALE RESOLUTION THEORY FOR ELASTIC MATERIAL WITH DAMAGE

LARS-ERIK LINDGREN[*], HAO QIN[*], WING KAM LIU[†] AND SHAN TANG[†]

[*]Luleå University of Technology
Engineering Sciences and Mathematics
971 87 Luleå, Sweden
e-mail: lars-erik.lindgren@ltu.se, www.ltu.se

[†]Northwestern University
Mechanical Engineering
2145 Sheridan Rd, Evanston, IL 60208-3111, USA
email : w-liu@northwestern.edu , www.tam.northwestern.edu

Key words: Multiscale, Damage, Localisation.

Abstract. The multiscale resolution continuum theory (MRCT) is a higher order continuum mechanics. A particle is represented by a point that is deformable. This enables the possibility to include the effect of microstructure features in the continuum model on the deformation behavior through additional nodal variables for the higher order scale. This reduces the need for a very fine mesh in order to resolve microstructure details. It is possible to further reduce the computational effort by keeping the additional degree of freedoms to a minimum by tailoring the theory to specific phenomena. The latter is illustrated in a simplified context for an elastic material with damage.

1 INTRODUCTION

The multiscale resolution continuum theory (MRCT) is a higher order continuum mechanics theory. It is a generalization of the micromorphic theory [1-3]. MRCT introduces length scales useful for application to localization problems. It has additional nodal parameters for the information about the deformation on the microstructural scale. This relieves the problem of having an extremely fine mesh. However, still very small elements are required and this together with the additional nodal variables adds to the computational burden. This paper demonstrates the method for an elastic material with brittle damage.

2 BACKGROUND

The multiscale approach belongs to the field of generalized continuum theories. Cosserat already 1909 introduced a generalized continuum. The Cosserat continuum, also named micropolar, introduced higher order terms. There are several papers [4-7] that describe different variants of generalized continuum theories. Eringen is the originator of the micromorphic theory and summarized his work in [1]. The micromorphic continuum includes the relative deformation of a subdomain at a specific point. Thus the particle represented by a

point is deformable. This enables the possibility to include the effect of microstructure features in the continuum model on the deformation behavior. The size of the subdomain determines a length scale l^i that influences the behavior at a given point. This domain is called a microdomain. The right superscript, i, denotes the level or scale of the microdomain as explained in the next section.

Eringen [1] indicated the possibility of formulating a theory for higher grades of continua but limited his description to the first grade. Germain [8] used a more elegant approach by utilizing the principle of virtual power. He showed how to include higher order terms in the deformation of the RVE. Liu with co-workers [9, 10] have developed a multiscale resolution continuum theory based on nested scales. The starting point for their derivation is also the principle of virtual power. The use of embedded RVEs or length scales facilitate the formulation of scales of higher order in the Multiscale Continuum Resolution Theory (MCRT).

3 MULTISCALE CONTINUUM RESOLUTION THEORY

The starting point for deriving the MCR theory is the principle of virtual power [11, 3, 10]. The internal virtual power is decomposed into a homogeneous and inhomogeneous part. The latter is due to the local stress variation within N nested RVEs within a point.

$$\delta p_{\text{int}}^{\text{hom}} + \delta p_{\text{int}}^{inh} = \sigma^0 : \delta \mathbf{l}^0 + \sum_{i=1}^{N} \int_{\Omega^i} \left({}_m\sigma^i : \delta {}_m\mathbf{l}^i - \sigma^0 : \delta \mathbf{l}^0 \right) d\Omega \tag{1}$$

, where $\mathbf{l}^0$ is the spatial velocity gradient and σ^0 is the Cauchy stress tensor on the macroscopic scale. The corresponding quantities, ${}_m\mathbf{l}^i$ and ${}_m\sigma^i$, are set up for each microdomain i. The scales are assumed to be separable so that ${}_m\mathbf{l}^i$ and ${}_m\sigma^i$ are constant for all smaller scales Ω^j, $j > i$. Eq. (1) is approximated to

$$\delta p_{\text{int}}^{\text{hom}} + \delta p_{\text{int}}^{inh} = \sigma^0 : \delta \mathbf{l}^0 + \sum_{i=1}^{N} \frac{1}{\Omega^i} \int_{\Omega^i} \left({}_m\beta^i : \left(\delta {}_m\mathbf{l}^i - \delta \mathbf{l}^0 \right) \right) d\Omega \tag{2}$$

A linear varying spatial velocity gradient within each subscale is assumed.

$${}_m\mathbf{l}^i \left(\mathbf{x} + \mathbf{y} \right) = \mathbf{l}^i \left(\mathbf{x} \right) + \mathbf{g}^i \left(\mathbf{x} \right) \cdot \mathbf{y}^i \tag{3}$$

where $\mathbf{y}^i$ is a local coordinate system at $\mathbf{x}$ in the microdomain. The term $\mathbf{l}^i$ gives the microstrain and $\mathbf{g}^i$ is its gradient. This leads after some manipulations to

$$\delta p_{\text{int}}^{\text{hom}} + \delta p_{\text{int}}^{inh} = \sigma^0 : \delta \mathbf{l}^0 + \sum_{i=1}^{N} \beta^i : \left(\delta \mathbf{l}^i - \delta \mathbf{l}^0 \right) + \mathbf{m}^i : \delta \mathbf{g}^i \tag{4}$$

where average microstresses are

$$\beta^i = \frac{1}{\Omega^i} \int_{\Omega^i} \beta_m^i \, d\Omega \tag{5}$$

and microcouples are

$$\mathbf{m}^i = \frac{1}{\Omega^i} \int_{\Omega^i} \beta_m^i \otimes \mathbf{y} \, d\Omega \tag{6}$$

Thus it is assumed that the microstresses and their couples can be related to the symmetric

part of the relative velocity gradient, $\mathbf{d}^i - \mathbf{d}^0$, and second velocity gradient $\mathbf{g}^i$, respectively. We use a hypoelastic approach. Notice that we limit the description to elastic deformations. The macroscopic stress update is written as

$$\sigma^{0\nabla} = \mathbf{C}_\sigma \mathbf{d}^0 \tag{7}$$

where $[\ ]^\nabla$ denotes an objective rate. $\mathbf{C}_\sigma$ is the elasticity tensor. The microstresses are updated by

$$\left(\beta^i\right)^\nabla = \mathbf{C}^i_\beta \left(\mathbf{d}^i - \mathbf{d}\right) + \mathbf{C}^i_{\beta m}\mathbf{g}^i \tag{8}$$

and the couples are updated by

$$\left(\mathbf{m}^i\right)^\nabla = \mathbf{C}^i_{\beta m} \left(\mathbf{d}^i - \mathbf{d}\right) + \mathbf{C}^i_{m}\mathbf{g}^i \tag{9}$$

Including the external virtual power and setting the total virtual power to zero leads to the following coupled equations of motion [3]

$$\begin{aligned} &\nabla\cdot\left(\sigma^0 - \sum_{i=1}^{N}\beta^i\right) = \rho\dot{\mathbf{v}}^0 \\ &\nabla\cdot\mathbf{m}^i - \beta^i = \gamma^i I^i \qquad i = 1..N \end{aligned} \tag{10}$$

where $\mathbf{v}^0$ is the macroscopic velocity field, ρ is the macroscopic density, ρ^i is the density in microdomain i, and γ^i is the micro-acceleration defined as

$$\gamma^i = \dot{\mathbf{l}}^i + \mathbf{l}^i\cdot\mathbf{l}^i \tag{11}$$

and the inertia tensor is

$$I^i = \frac{1}{\Omega^i}\int_{\Omega^1}\rho^i\mathbf{y}^i\otimes\mathbf{y}^i d\Omega \tag{12}$$

4 SIMPLIFIED MCRT FOR ELASTIC-DAMAGE MODEL

It is possible to reduce the computational cost by adapting the theory to specific phenomena. Kadowaki and Liu [12] demonstrated this for the case of granular media. We are here considering an elastic material with local softening/fracture with one additional scale (N=1). Elastic behavior is assumed. The damaged regionin the microdomain, gray in Figure 1, is assumed to completely lose its strength. Then homogenized the constitutive equation is

$$\mathbf{C}^1_\beta = \frac{1}{\Omega^1}\int_{\Omega^1}\mathbf{C}_\sigma d\Omega = \mathbf{C}_\sigma\left(1-\omega\right) \tag{13}$$

where ω is the fraction of the damaged volume in the microdomain. The coupling matrix may be non-zero when the damage is unsymmetric in the microdomain. We assume it is symmetric and thus have

$$\mathbf{C}^1_{\beta m} = \frac{1}{\Omega^1}\int_{\Omega^1}\mathbf{C}_\sigma\otimes y^1 d\Omega = \mathbf{0} \tag{14}$$

The constitutive matrix for the couple terms becomes

$$\mathbf{C}^1_m = \mathbf{C}^e_\sigma\otimes\frac{\left(l^1\right)^2}{12}\mathbf{D} \tag{15}$$

where

$$\mathbf{D} = \begin{bmatrix} (Z_1)^3 Z_2 Z_3 & 0 & 0 \\ 0 & Z_1 (Z_2)^3 Z_3 & 0 \\ 0 & 0 & Z_1 Z_2 (Z_3)^3 \end{bmatrix} \tag{16}$$

with

$$\mathbf{Z}_i^1 = \frac{y_i^+ + y_i^-}{l^1} = \frac{2y_i}{l^1} \tag{17}$$

The parameters $y_i^{\pm}$ are the distances from origin to where damage has reached into the microdomain, see Figure 1. We have symmetric damage in the current one-dimensional implementation, ie. $y_i^+ = y_i^-$. The damage can be unsymmetric for when several stress or strain components are used. The subscript *i* denotes the coordinate direction of the normal to this surface.

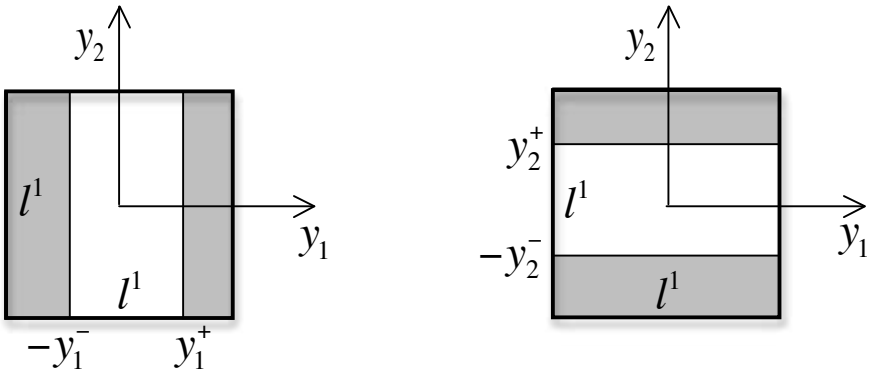

Figure 1: Two-dimensional view of damage volumes (gray) that are growing into the microdomain.

The fraction of damage volume is

$$\omega = \prod_{i=1}^{R} \left(1 - \frac{2y_i}{l^1}\right) \tag{18}$$

where *R* is the number of dimensions of the problem. We have R=1 in the case below. Damage is assumed to be due to the volumetric deformation in the microdomain. Therefore, all shear components of higher order degree of freedoms are excluded. The reduced microstress/deformation are

$$\begin{aligned} \beta^1 &= \begin{bmatrix} \beta_{11}^1 & \beta_{22}^1 & \beta_{33}^1 \end{bmatrix}^T \\ \mathbf{d}^1 &= \begin{bmatrix} d_{11}^1 & d_{22}^1 & d_{33}^1 \end{bmatrix}^T \end{aligned} \tag{19}$$

and the corresponding couples/gradients are reduced to

$$\begin{aligned} \mathbf{m}^1 &= \begin{bmatrix} m_{111}^1 & m_{112}^1 & m_{113}^1 & m_{221}^1 & m_{222}^1 & m_{223}^1 & m_{331}^1 & m_{332}^1 & m_{333}^1 \end{bmatrix}^T \\ \mathbf{g}^1 &= \begin{bmatrix} d_{11,1}^1 & d_{11,2}^1 & d_{11,3}^1 & d_{22,1}^1 & d_{22,2}^1 & d_{22,3}^1 & d_{33,1}^1 & d_{33,2}^1 & d_{33,3}^1 \end{bmatrix}^T \end{aligned} \tag{20}$$

Computing the gradients from the first derivatives of the microstrain over a finite element reduces the number of independent nodal degrees of freedom (dof) further. Thus the three

dimensional finite element will have six (three displacements and three normal microstrains) unknowns for each node. The one-dimensional example below has only two dofs per node.

Different damage criterion can be applied. A simple linear increase in damage when the macroscopic strain exceeds a given criterion and the damage becomes complete ($\omega = 1$) when a fracture strain is reached.

5 FINITE ELEMENT IMPLEMENTATION

The implementation of the above outlined theory is shown for a one-dimensional rod with two nodes.

5.1 Kinematics

The finite element interpolation of nodal velocities and rate of microstrains is written as

$$\mathbf{v}(\mathbf{x}) = \begin{bmatrix} N_1^0 & N_2^0 & 0 & 0 \\ 0 & 0 & N_1^1 & N_2^1 \end{bmatrix} \begin{bmatrix} v_{x1} \\ v_{x2} \\ d^1_{xx1} \\ d^1_{xx2} \end{bmatrix} = \begin{bmatrix} \mathbf{N}^0 & 0 \\ 0 & \mathbf{N}^1 \end{bmatrix} \begin{bmatrix} \mathbf{v}^0 \\ \mathbf{d}^1 \end{bmatrix} = \mathbf{N}\mathbf{v} \tag{21}$$

N_n^0 and N_n^1 indicates that we may use different functions to interpolate the microstrain than the nodal velocity, or use different number of integration points when evaluating them. This is not utilized in the following.

The gradient of microstrain is computed as

$$\mathbf{g}^1(\mathbf{x}) = g^1_{xxx} = d^1_{xx,x} = \begin{bmatrix} \dfrac{\partial N_1^1}{\partial x} & \dfrac{\partial N_2^1}{\partial x} \end{bmatrix} \begin{bmatrix} d^1_{xx1} \\ d^1_{xx2} \end{bmatrix} = \mathbf{B}^1\mathbf{d}^1 \tag{22}$$

The macroscopic spatial velocity gradient is obtained by

$$\mathbf{d}^0(\mathbf{x}) = d^0_{xx} = \begin{bmatrix} \dfrac{\partial N_1^0}{\partial x} & \dfrac{\partial N_2^0}{\partial x} \end{bmatrix} \begin{bmatrix} v_{x1} \\ v_{x2} \end{bmatrix} = \mathbf{B}^0\mathbf{v}^0 \tag{23}$$

The needed rates of the macroscopic strain, microstrain and its gradient can now be written as

$$\begin{aligned} \mathbf{d}^0(\mathbf{x}) &= \mathbf{B}^0\mathbf{v}^0 \\ \mathbf{d}^1(\mathbf{x}) &= \mathbf{N}^1\mathbf{d}^1 \\ \mathbf{g}^1(\mathbf{x}) &= \mathbf{B}^1\mathbf{d}^1 \end{aligned} \tag{24}$$

The generalized strain rate vector is introduced

$$\Delta(\mathbf{x}) = \begin{bmatrix} \mathbf{d}^0(\mathbf{x}) \\ \mathbf{d}^1(\mathbf{x}) - \mathbf{d}^0(\mathbf{x}) \\ \mathbf{g}^1(\mathbf{x}) \end{bmatrix} = \begin{bmatrix} \mathbf{B}^0 & 0 \\ -\mathbf{B}^0 & \mathbf{N}^1 \\ 0 & \mathbf{B}^1 \end{bmatrix} \begin{bmatrix} \mathbf{v}^0 \\ \mathbf{d}^1 \end{bmatrix} = \mathbf{Q}\mathbf{v} \tag{25}$$

5.2 Kinetics

Kinetic variables that are energy conjugate kinetic with those in Eq. (25) are

$$\Sigma = \begin{bmatrix} \sigma_x^0 \\ \beta_{xx}^1 \\ m_{xxx}^1 \end{bmatrix} \tag{26}$$

Their (objective) rates are obtained from the constitutive model as described below. We want to continuously update their values, as they are needed for the internal force calculations.

5.3 Constitutive equations

We specialize the matrices in section 4 for the uniaxial stress case. Then we have

$$\sigma_{xx}^{\nabla} = \mathbf{C}_o \mathbf{d}^0 \Leftrightarrow \dot{\sigma}_{xx}^0 = E d_{xx}^0 \tag{27}$$

The higher order constitutive relations are given by

$$\left(\beta^1\right)^{\nabla} = \mathbf{C}_\beta^1 \left(\mathbf{d}^1 - \mathbf{d}\right) + \mathbf{C}_{\beta m}^1 \mathbf{g}^1 \Leftrightarrow \dot{\beta}_{xx}^1 = C_\beta^1 \left(d_{xx}^1 - d_{xx}^0\right) + C_{\beta m}^1 g_{xxx}^1 \tag{28}$$

and

$$\left(\mathbf{m}^1\right)^{\nabla} = \mathbf{C}_{\beta m}^1 \left(\mathbf{d}^1 - \mathbf{d}\right) + \mathbf{C}_m^1 \mathbf{g}^1 \Leftrightarrow \dot{m}_{xxx}^1 = C_{\beta m}^1 \left(d_{xx}^1 - d_{xx}^0\right) + C_m^1 g_{xxx}^1 \tag{29}$$

The objective rates are equal to time rates in case of one-dimensional formulation, as we have no rotations. The microdomain properties are calculated based on assuming elastic behavior and a damaged zone without and stiffness. Symmetry of damaged region gives

$$C_{\beta m}^1 = \frac{1}{l^1} \int_{-y_1^-}^{y_1^+} E^1 y^1 dy^1 = \left[\text{as } y_1^+ = y_1^- = y_1\right] = 0 \tag{30}$$

The microstrain elasticity is

$$\mathbf{C}_\beta^1 = \frac{1}{l^1} \int_{-y_1^-}^{y_1^+} E^1 dy = E^1 \frac{\left(y_1^+ + y_1^-\right)}{l^1} = E^1 \frac{2y_1}{l^1} = E^1 \left(1 - \omega\right) \tag{31}$$

where it has been used that the fraction of damage material, ω ,is

$$\left(1 - \omega\right) = \frac{2y_1}{l^1} \tag{32}$$

The microcouple constitutive relation is

$$C_m^1 = \frac{1}{l^1} \int_{-y_1^-}^{y_1^+} E^1 \left(y^1\right)^2 dy^1 = \left[y_1^+ = y_1^- = y_1\right] = \frac{E^1 \left(l^1\right)^2}{12} \left(2 \frac{y_1}{l^1}\right)^3 = \frac{E^1 \left(l^1\right)^2}{12} \left(1 - \omega\right)^3 \tag{33}$$

The extended constitutive matrix becomes then

$$\Sigma^{\nabla} = \begin{bmatrix} E^0 & 0 & 0 \\ 0 & E^1 \left(1 - \omega\right) & 0 \\ 0 & 0 & \dfrac{E^1 \left(l^1\right)^2}{12} \left(1 - \omega\right)^3 \end{bmatrix} \Delta = \mathbf{C} \Delta \tag{34}$$

5.4 Element internal force vector

The internal forces are computed as

$$\mathbf{f}_{\text{int}} = \begin{bmatrix} f_1^0 \\ f_2^0 \\ f_1^1 \\ f_2^1 \end{bmatrix} = \int_{V^e} \mathbf{Q}^T \Sigma \, dV = \int_{x_1}^{x_2} \begin{bmatrix} \frac{\partial N_1^0}{\partial x} & -\frac{\partial N_1^0}{\partial x} & 0 \\ \frac{\partial N_2^0}{\partial x} & -\frac{\partial N_2^0}{\partial x} & 0 \\ 0 & N_1^1 & \frac{\partial N_1^1}{\partial x} \\ 0 & N_2^1 & \frac{\partial N_2^1}{\partial x} \end{bmatrix} \begin{bmatrix} \sigma^0 \\ \beta^1 \\ m^1 \end{bmatrix} a \, dx \tag{35}$$

Where a is the area of the cross-section of the rod. The internal forces can be split it up into macroscopic forces and microscopic forces

$$\mathbf{f}_{\text{int}}^0 = \begin{bmatrix} f_1^0 \\ f_2^0 \end{bmatrix} = \int_{x_1}^{x_2} \begin{bmatrix} \frac{\partial N_1^0}{\partial x}\left(\sigma^0 - \beta^1\right) \\ \frac{\partial N_2^0}{\partial x}\left(\sigma^0 - \beta^1\right) \end{bmatrix} a dx \tag{36}$$

respectively

$$\mathbf{f}_{\text{int}}^1 = \begin{bmatrix} f_1^1 \\ f_2^1 \end{bmatrix} = \int_{x_1}^{x_2} \begin{bmatrix} N_1^1 \beta^1 + \frac{\partial N_1^1}{\partial x} m^1 \\ N_2^1 \beta^1 + \frac{\partial N_2^1}{\partial x} m^1 \end{bmatrix} a dx \tag{37}$$

5.5 Element tangent stiffness matrix

The tangent stiffness matrix is

$$\mathbf{K} = \frac{d\left(\mathbf{F}_{\text{int}} - \mathbf{F}_{\text{ext}}\right)}{d\mathbf{V}} = \frac{d\mathbf{F}_{\text{int}}}{d\mathbf{V}} \tag{38}$$

where $\mathbf{F}_{\text{int}}$ is the global internal force vector and $\mathbf{F}_{\text{ext}}$ is the external forces. $\mathbf{V}$ is the global vector of nodal values corresponding $\mathbf{v}$ in Eq. (20). It is approximated by computing the element contribution as

$$\mathbf{k} = \frac{d\left(\mathbf{f}_{\text{int}}\right)}{d\mathbf{v}} = \frac{d\mathbf{f}_{\text{int}}}{d\mathbf{v}} \approx \int_{V^e} \mathbf{Q}^T \frac{d\Sigma}{d\Delta} \mathbf{Q} dV \tag{39}$$

where

$$\frac{d\Sigma}{d\Delta} = \begin{bmatrix} E^0 & 0 & 0 \\ 0 & E^1\left(1-\omega\right) & 0 \\ 0 & 0 & \frac{E^1\left(l^1\right)^2}{12}\left(1-\omega\right)^3 \end{bmatrix} \tag{40}$$

We use a fixed damage during an increment and update between the increments. This requires small time steps but removes this nonlinearity from the iterative process and simplifies the derivation of the consistent constitutive matrix in Eq. (39). The stiffness matrix can be split into three separate contributions. The macroscopic part is

$$\mathbf{k}^0 = \int_{x_1}^{x_2} E^0 \begin{bmatrix} \left(\frac{\partial N_1^0}{\partial x}\right)^2 & \frac{\partial N_1^0}{\partial x}\frac{\partial N_2^0}{\partial x} & 0 & 0 \\ \frac{\partial N_1^0}{\partial x}\frac{\partial N_2^0}{\partial x} & \left(\frac{\partial N_2^0}{\partial x}\right)^2 & 0 & 0 \\ 0 & 0 & 0 & 0 \\ 0 & 0 & 0 & 0 \end{bmatrix} a\,dx \tag{41}$$

The coupling matrix is

$$\mathbf{k}^{01} = \int_{x_1}^{x_2} E^1(1-\omega) \begin{bmatrix} \left(\frac{\partial N_1^0}{\partial x}\right)^2 & \frac{\partial N_1^0}{\partial x}\frac{\partial N_2^0}{\partial x} & -\frac{\partial N_1^0}{\partial x}N_1^1 & -\frac{\partial N_1^0}{\partial x}N_2^1 \\ \frac{\partial N_1^0}{\partial x}\frac{\partial N_2^0}{\partial x} & \left(\frac{\partial N_2^0}{\partial x}\right)^2 & -\frac{\partial N_2^0}{\partial x}N_1^1 & -\frac{\partial N_2^0}{\partial x}N_2^1 \\ -\frac{\partial N_1^0}{\partial x}N_1^1 & -\frac{\partial N_2^0}{\partial x}N_1^1 & \left(N_1^1\right)^2 & N_1^1 N_2^1 \\ -\frac{\partial N_1^0}{\partial x}N_2^1 & -\frac{\partial N_2^0}{\partial x}N_2^1 & N_1^1 N_2^1 & \left(N_2^1\right)^2 \end{bmatrix} a\,dx \tag{42}$$

The higher order contribution is

$$\mathbf{k}^1 = \int_{x_1}^{x_2} \frac{E^1\left(l^1\right)^2}{12}(1-\omega)^3 \begin{bmatrix} 0 & 0 & 0 & 0 \\ 0 & 0 & 0 & 0 \\ 0 & 0 & \left(\frac{\partial N_1^1}{\partial x}\right)^2 & \frac{\partial N_1^1}{\partial x}\frac{\partial N_2^1}{\partial x} \\ 0 & 0 & \frac{\partial N_1^1}{\partial x}\frac{\partial N_2^1}{\partial x} & \left(\frac{\partial N_2^1}{\partial x}\right)^2 \end{bmatrix} a\,dx \tag{43}$$

6 RESULTS

The formulation in the previous section has been implemented in Matlab™. A rod is subject to tension by prescribing opposite motions of each end. The microstress β_{xx}^1 is set to zero at the ends, ie microstrain is equal to the macroscopic strain there. The used properties are given in Table 1. A simple damage model is used. It is

$$\omega = \left\langle \frac{\varepsilon^0 - \varepsilon_{init}}{\varepsilon_{fracture} - \varepsilon_{init}} \right\rangle \tag{44}$$

The symbol $\langle\ \rangle$ denotes that the expression is zero for negative arguments. The damage is only applied in the center region of the rod, $x \in [-0.005L, 0.005L]$. x is the coordinate of the integration point at the center of the element. The model is set up so that there is always one element centered around x=0.

The macroscopic stress for the problem follows the analytic solution

$$\sigma^0 = E^0 \ln\left(1 + \frac{u}{L}\right) \tag{45}$$

where u is the total elongation of the rod and L=0.1 m is its initial length. The logarithmic strain definition has been used.

The results below are plotted at different instances in time. The strain computed according to Eq. (44) is 0.0, 0.26, 0.47, 0.64, 0.79, 0.91, 1.03, 1.13, 1.31 and 1.39 for each of the lines, respectively. The macroscopic strain and stress are shown in Figure 2. All plots are based on averaged nodal values when they show element data. The number of elements was 101 and the center element is subject to damage. The overall strain and stress follow the analytic solution. The localization in the center element is obvious. The micro-stress and damage can be seen in Figure 3. The damage weakens the microdomain and the micro-stress decreases.

Splitting the element in the centre of the rod into four elements gives

Table 1: Used material properties

E^0	2.10^{11} Pa
E^1	$= E^0$
l^1	$2.\ 10^{-6}$ m
ε_{init}	0.05
$\varepsilon_{fracture}$	0.30

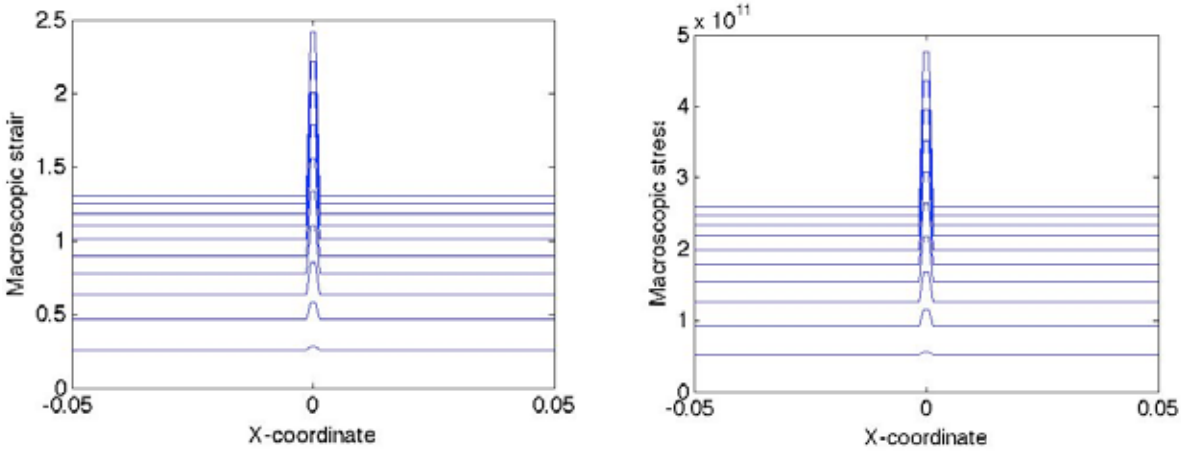

Figure 2: Macroscopic strain and stress during loading.

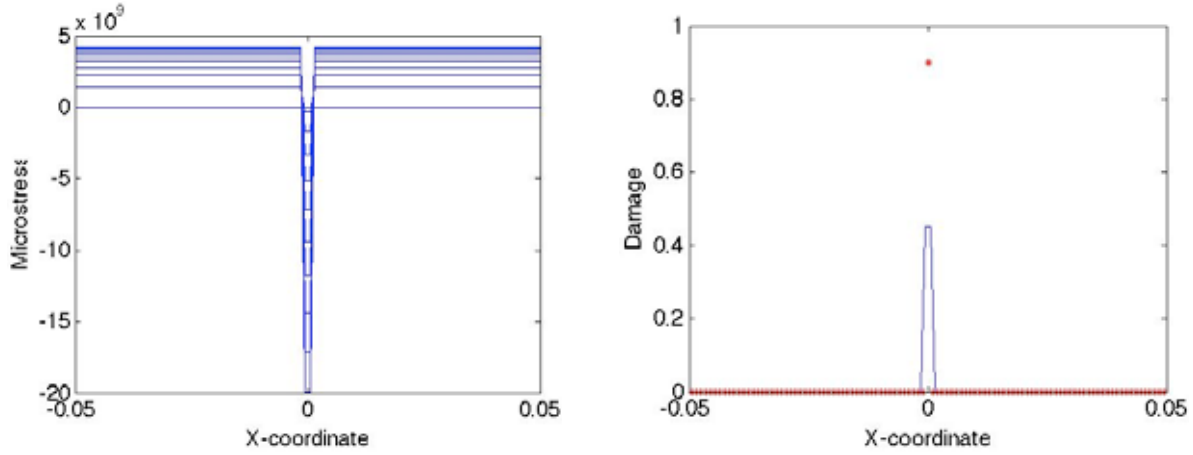

Figure 3: Micro-stress and damage during loading. The crosses in the damage plot denote values at element center. There it can be seen that the damage reaches 0.9.

7 DISCUSSIONS

Hardening and softening behavior of materials depends in a wide range of scales. Despite this, macroscopic models have been successfully used to describe the hardening behavior of materials. However, softening behavior that is determined by the weakest link in the material poses a challenge for these models. Model that brings in a length scale is one step forward in creating convergent finite element models. The MCRT is an approach that does this and also reduces the need for a very fine mesh in the localization zone. However, this is at the additional cost of additional nodal degree of freedoms. Therefore, it is of particular interest to develop constitutive models for the microdomain with a minimum of higher order degrees of freedoms for specific problems. The preliminary evaluated damage model is one example. The convergence behavior of the model need be evaluated as well as the effect on the condition number of the stiffness matrix for different combinations of element sizes and size of microdomain.

ACKNOWLEDGMENTS

The L-E Lindgren would like to acknowledge the financial support from the Steel Research Programme of the Swedish Steel Producers Association (Jernkontoret) financed by the Swedish Agency for Innovative Systems (VINNOVA) and Sandvik Materials Technology (SMT) together with Swedish Steel (SSAB). H Qin has been financially supported by the Centre of High-performance Steel (CHS). WK Liu and S Tang are supported by NSF CMMI Grant 0823327 and the ARO.

REFERENCES

[1] Eringen, A., *Microcontinuum field theories. I: Foundations and solids.*, Springer Verlag, (1997).
[2] Kadowaki, H. and Liu, W., A multiscale approach for the mircopolar continuum model, *Computer Methods in Engineering & Sciences* (2005) **7**:269-282.
[3] Vernerey, F., Liu, W. K. and Moran, B., Multi-scale micromorphic theory for hierarchical

materials, *Journal of the Mechanics and Physics of Solids* (2007) **55**:2603-2651.
[4] Skatulla, S., Arockiarajan, A. and Sansour, C., A nonlinear generalized continuum approach for electro-elasticity including scale effects, *Journal of the Mechanics and Physics of Solids* (2009) **57**:137-160.
[5] Lazar, M. and Maugin, G. A., On microcontinuum field theories: The eshelby stress tensor and incompatibility conditions, *Philosophical Magazine* (2007) **87**:3853 - 3870.
[6] Forest, S., Micromorphic approach for gradient elasticity, viscoplasticity, and damage, *Journal of Engineering Mechanics* (2009) **135**:117-131.
[7] Lakes, R., Experimental methods for study of cosserat solids and other generalized elastic continua, *Continuum models for materials with micro-structure*, H. Mulhaus (Editor), J. Wiley, (1995).
[8] Germain, P., The method of virtual power in continuum mechanics. Part 2: Microstructure, *SIAM Journal on Applied Mathematics* (1973) **25**:556-575.
[9] Liu, W. and McVeigh, C., Predictive multiscale theory for design of heteregeneous materials, *Computational Mechanics* (2008) **42**:147-170.
[10] Vernerey, F. J., Liu, W. K., Moran, B. and Olson, G., A micromorphic model for the multiple scale failure of heterogeneous materials, *Journal of the Mechanics and Physics of Solids* (2008) **56**:1320-1347.
[11] McVeigh, C. and Liu, W. K., Multiresolution modeling of ductile reinforced brittle composites, *Journal of the Mechanics and Physics of Solids* (2009) **57**:244-267.
[12] Kadowaki, H. and Liu, W., A multiscale approach for the micropolar continuum model, *Computer. Modeling in Engineering & Sciences* (2005) **7**:269-282.